Revista Internacional de Ciencia y Tecnología de la Información Geográfica
International Review of Geographical Information Science and Technology

Del Valle, H., Hardtke, L., Blanco, P. y Sione, W. (2013): "Assessment of land degradation Using Shannon entropy Approach On Polsar Images In Patagonian Coastal deserts", GeoFocus (Artículos), nº13-2, p. 84-111. ISSN: 1578-5157

ASSESSMENT OF LAND DEGRADATION USING SHANNON ENTROPY APPROACH ON POLSAR IMAGES IN PATAGONIAN COASTAL DESERTS

HÉCTOR DEL VALLE[1], LEONARDO HARDTKE[1], PAULA BLANCO[1], WALTER SIONE[2,3]
[1] Centro Nacional Patagónico (CENPAT),
Consejo Nacional de Investigaciones Científicas y Técnicas (CONICET).
Boulevard Almirante Brown 2915, CP 9120 Puerto Madryn, Chubut, Argentina.
delvalle@cenpat.edu.ar, leohardtke@cenpat.edu.ar, blanco@cenpat.edu.ar
[2] Centro Regional de Geomática (CEREGEO), Facultad de Ciencia y Técnica (FCyT),
Universidad Autónoma de Entre Ríos (UADER).
España y Materi SN, CP 3105 Diamante, Entre Ríos, Argentina.
[3] PRODITEL, Universidad Nacional de Luján (UNLu).
Cruce de rutas 5 y ex 7, CP 6700 Luján, Buenos Aires, Argentina.
sione@ceregeo.org.ar

ABSTRACT

We focus on Shannon Entropy (*SE*) for the characterization of polarimetric Synthetic Aperture Radar (PolSAR) images. This approach analyzes the information contribution made by individual pixels to the whole image for assessment of land degradation in the information content of ALOS PALSAR images. Additionally, the performance of other polarization parameters, and polarization decomposition is illustrated and discussed. Dual-Pol and Quad-Pol scenes have been acquired under the SAOCOM (Satélite Argentino de Observación con Microondas, Spanish for Argentine Microwaves Observation Satellite) project in 2010 and 2011, from northeastern Patagonian coastal desert, Argentina. The accuracy of the *SE* map was assessed using a set of ground observations based on remotely sensed data that have higher accuracy. The results show that the *SE* can describe and determine the image features more obviously in the study area, so that it represents an important reference value for land degradation detection and land status characteristics extraction.

Keywords: Polarimetric key parameters, burned areas, wind-driven land degradation, overgrazing, desertification.

Recibido: 22/02/2013
Aceptada versión definitiva: 26/06/2013

Del Valle, H., Hardtke, L., Blanco, P. y Sione, W. (2013): "Assessment of land degradation Using Shannon entropy Approach On Polsar Images In Patagonian Coastal deserts", GeoFocus (Artículos), nº13-2, p. 84-111. ISSN: 1578-5157

EVALUACIÓN DE LA DEGRADACIÓN DE LA TIERRA USANDO LA ENTROPÍA DE SHANNON SOBRE IMÁGENES POLARIMÉTRICAS EN DESIERTOS COSTEROS PATAGÓNICOS

RESUMEN

En esta investigación se focalizó en la Entropía de Shannon (*ES*) para la caracterización de imágenes polarimétricas de apertura sintética. Este parámetro analiza la contribución de la información por pixeles individuales para toda la imagen en la evaluación de la degradación de la tierra en imágenes ALOS PALSAR. Escenas de polarización dual y cuádruple fueron adquiridas bajo el proyecto SAOCOM (Satélite Argentino de Observación con Microondas) en 2010 y 2011, del desierto costero noreste patagónico, Argentina. Los mapas fueron verificados con información de alta verosimilitud para la misma área de estudio. Los resultados muestran que la *ES* puede describir y precisar las características de las imágenes de manera obvia, de tal manera que representa un valor de referencia para la detección de la degradación de la tierra y la extracción de las características de los diferentes estados y transiciones.

Palabras clave: Parámetros polarimétricos clave, áreas quemadas, degradación eólica de la tierra, sobrepastoreo, desertificación.

1. Introduction

For more than four decades remote sensing images have been used to monitoring and understanding the desert biomes (Tueller & Lorain, 1973; Barrett & Hamilton, 1986; Sahai, 1993; Cohen & Goward, 2004; Mulder, *et al.*, 2011). Because of large data availability, optical images have been used both in research and operational basis. On the other hand, microwave remote sensing is of significantly useful due mostly to low soil moisture content and homogeneous and temporally stable distribution of dielectric constant. Thus, temporal variability of scattering and emission from targets are mainly a function of geometrical characteristics.

Studies over the last 30 years with different Synthetic Aperture Radar (SAR) sensors, led to significant advances mostly in elevation modeling, sand penetration, geology, morphology and dynamics of sand dunes (Greeley *et al.*, 1997; Schaber & Breed, 1999; Blumberg, 2006; Hugenholtz *et al.*, 2012). Although the interaction between polarized microwaves and desert targets has been studied widely, far less is understood about the added information provided from polarimetric SAR. Polarimetric data could provide advantages, specifically an improved sensitivity to identify signals of environmental changes leading to desertification, and also recognizing how soil erosion negatively impacts on rangeland production, farm infrastructure, and ecosystem health (del Valle *et al.*, 2010).

Ray *et al.* (1992) using multispectral radar images (AIRSAR) on agricultural lands validated the usefulness of polarimetric techniques supported by limited field work for study of land degradation at synoptic scales. These authors concluded that polarimetric SAR can be used to detect wind-formed features associated with desertification. However, many new questions have been raised and many still remain unanswered, specifically the spectral similarity among surface

Del Valle, H., Hardtke, L., Blanco, P. y Sione, W. (2013): "Assessment of land degradation Using Shannon entropy Approach On Polsar Images In Patagonian Coastal deserts", GeoFocus (Artículos), nº13-2, p. 84-111. ISSN: 1578-5157

component associated with land degradation, and the one-to-many relationship between surface features and land degradation processes. There is limited availability of polarimetric data to evaluate the robustness of the classifications with different land degradation status and cause-to-cover situations.

Shannon Entropy (*SE*) is one of the polarimetric key parameters that measures the statistical disorder of the medium illuminated by the radar, and it is a sum of three contributions related to intensity, polarimetry and interferometry (Morio *et al.*, 2008). It reflects that *SE* measured from polarimetric and interferometric SAR datasets contains valuable information which can be used in remote sensing problems (Morio *et al.*, 2008; Bian *et al.*, 2011). This would allow determining polarimetric intra class properties in different regions of an image for detailed land cover and land use relationships.

We analyze the application of *SE* (intensity and polarimetry), as well as other polarization parameters, and polarization decomposition results in multimodal ALOS PALSAR images. We choose *SE* approach because it seems especially well adjusted in the field of image analysis (classification results in terms of radiometric and spatial entropy), where statistical properties control signal and noise.

2. Materials and methods

2.1. Study area and environmental features

Our test sites are located in northeastern Patagonia, on the east coast of the Río Negro province and northeastern coast of that of Chubut, Argentina, centered at 42º 02´23"S, 64º 13´24"W. The study area is surrounded by the San Matías, San José and Nuevo Gulfs, and the Atlantic Ocean to the east and south. Figure 1A-B show the study cases on the map of Vegetation Continuous Field (VCF) from Patagonia region (1A, Hansen *et al.*, 2003) and on Digital Elevation Model (1B, SRTM 30-m). Each site covers an area of approximately 5,733 sq. km (Río Negro) and 9,240 sq. km (Chubut). The test sites have extensive supporting data both in terms of in-situ measurements and also supporting Earth Observation datasets (Rostagno, 1981; González Díaz & Malagnino, 1984; del Valle *et al.*, 2000, 2008 and 2010; Ayesa *et al.*, 2002, and Blanco *et al.*, 2008).

Del Valle, H., Hardtke, L., Blanco, P. y Sione, W. (2013): "Assessment of land degradation Using Shannon entropy Approach On Polsar Images In Patagonian Coastal deserts", GeoFocus (Artículos), nº13-2, p. 84-111. ISSN: 1578-5157

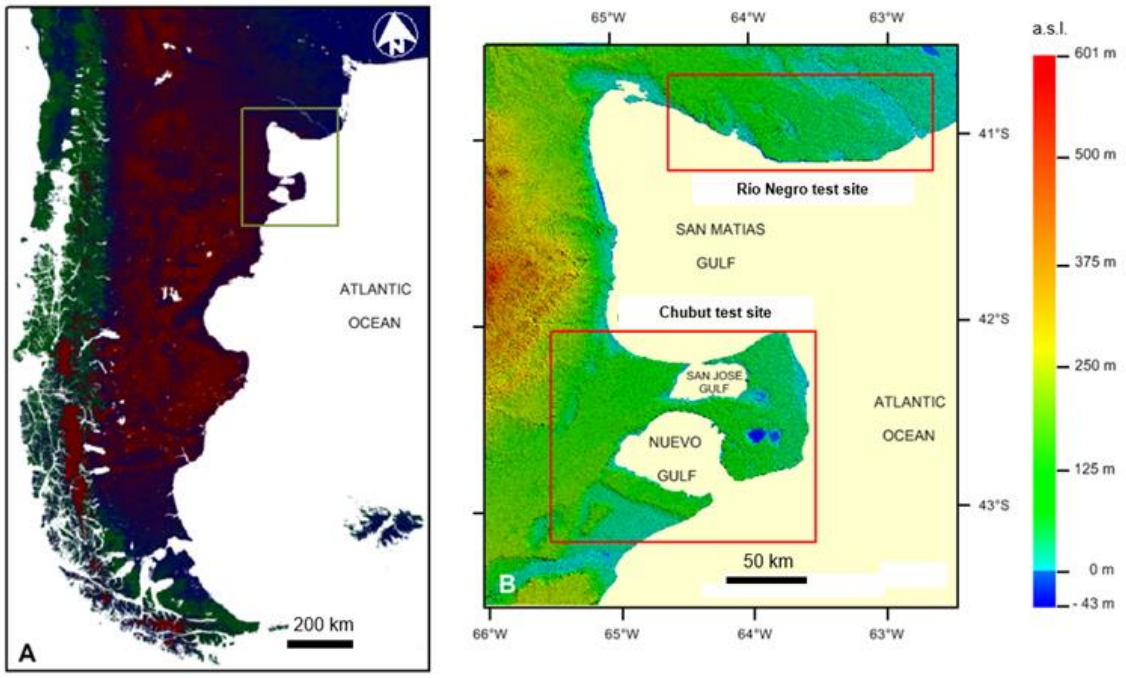

Figure 1A-B. 1A. Vegetation Continuous Fields (VCF) from Patagonia (Chile-Argentina) contains proportional estimates for vegetative cover types: bare ground (red), woody vegetation (green), and shrub-herbaceous vegetation (blue). Source: Collection 3, University of Maryland, Hansen *et al.* (2003). 1B. Map of the study region showing the altitude above sea level (m) in northeastern Patagonia (Argentina). This figure was extracted from the SRTM 30-m (Source: CONAE). The red rectangles represent the location of the ALOS-PALSAR test sites.

Table 1 summarizes the principal environmental features of the test sites. The climate is temperate arid. The proximity to the sea influences the climate especially in reducing the annual temperature amplitude, the number of days of frost, and the interannual rainfall fluctuations (Barros & Rivero, 1982; Coronato, 1992). From the overall ecological viewpoint, this coastal ecosystem could be considered like a semidesert. There is no clearly defined rain season in the area. However, rainfall is more frequent in autumn and winter. The test sites share with the rest of Patagonia the same windy conditions, with an annual mean wind speed >4.0 ms^{-1}. However, westerly winds are less predominant here, while north and northeast winds become more frequent because of the stronger influence of the southwest Atlantic anticyclone (Paruelo *et al.*, 1998). Spring is progressively warmer but may be extremely windy.

Del Valle, H., Hardtke, L., Blanco, P. y Sione, W. (2013): "Assessment of land degradation Using Shannon entropy Approach On Polsar Images In Patagonian Coastal deserts", GeoFocus (Artículos), nº13-2, p. 84-111. ISSN: 1578-5157

Table 1. Environmental and structural characteristics of the test sites studied

Environmental features	Test Sites	
	Chubut	**Río Negro**
Mean annual precipitation (mm) [1]	231	325
Mean annual temperature (ºC) [1]	13.0	14.5
Mean annual wind speed (m s^{-1}) [2]	7.2	4.5
Maximum annual wind speed distribution [2]	spring (September) and summer (January)	
Wind direction (cardinal directions) [2]	N and SW	NW and SW
Aridity index [3]	0.20	0.27
Landforms [4]	Stabilized dunefields, active sand dunes, interdune scald-scabby, blowouts, discontinuous aeolian mantles, gravel plains, depressions, foreshore sand beaches, cliffs scarps, tidal salt marshes, tidal flats, fluvial landforms of streams, stream beds and river valley (Río Negro test site)	
Vegetation types [5]	Shrubs/scrubs, grasses, mosaics, salt flat, barren land	Shrubs/scrubs, woods, grasses, croplands, mosaics, salt flat, barren land
Dominant Soils [6]	AR, RG, CL, CM, PL, LP, SC, SN	AR, RG, CL, CM, LP, PL, SC, SL, FL, PH, VR
Land Use [5]	Rangelands (herbaceous, shrubs, mixed)	Rangelands (herbaceous, woods, shrubs, mixed), Agricultural land (cropland and pasture)

[1] Paruelo *et al*. (1998); [2] Barros (1986); [3] Bioclimatic zones defined by Le Houérou (1996): Arid (0.05-0.20), Semiarid (0.20-0.45); [4] González Díaz (1981); [5] Ayesa *et al*. (2002); [6] World Reference Base for soil resources (WRB): AR (Arenosol), CL (Calcisol), CM (Cambisol), FL (Fluvisol), LP (Leptosol), PH (Phaeozem), PL (Planosol), RG (Regosol), SC (Solonchak), SN (Solonetz), VR (Vertisol).

Gravel deposits of Pliocene-Pleistocene age, locally named "Rodados Patagónicos", cover parts of the test sites. Tertiary (Miocene) marine and/or continental sediments are exposed on the seashore cliffs and in the erosion fronts of tectonic depressions. Our study area includes gravel plains and sand deposits (Haller *et al.*, 2000). Besides, it is included within the aeolian unit named northern Patagonia and southern Pampean sand mantles and dunefields (Zárate & Tripaldi, 2012). However, these authors restrict the limits of this aeolian unit, that for us, it is much more extensive, comprising also the northeastern Chubut province (del Valle *et al.*, 2010). The test sites are affected by the progression of fronts of active sand dunes grouped in discrete megapatches. Dune mobility is high because of prevailing strong winds that cause eastward sand migration (del Valle *et al.*, 2008). Air circulation is strongly influenced by the shape of the coastline, while the dunefields are very

Del Valle, H., Hardtke, L., Blanco, P. y Sione, W. (2013): "Assessment of land degradation Using Shannon entropy Approach On Polsar Images In Patagonian Coastal deserts", GeoFocus (Artículos), nº13-2, p. 84-111. ISSN: 1578-5157

much related to the loose sediments of these windward coasts that are unique cases in the whole Patagonia according to the main orientation of the shoreline.

2.2. Data sources

Dual and quad polarimetric ALOS/PALSAR data acquired in 2010 and 2011 were analyzed (table 2). PALSAR is an enhanced version of the SAR on board JERS, developed by JAXA and METI, Japan (Rosenqvist *et al.*, 2007). Level 1.1 products lack map projection record and geolocation data for each line (data in signal data format, not processed, where geolocation could be included).

Table 2. ALOS PALSAR datasets

Acquisition date	Orbit	Level	Format	Imaging Mode	Azimuth/ range resolution m	Inc. angle of image center degree	Orbit pass
Río Negro test site							
21-JUL-2010	23923	1.1	SLC	FBD	3.2/14.9	38.9	Ascending
19-AUG-2010	24346					39.0	
05-SEP-2010	24594					38.9	
22-SEP-2010	24842						
26-NOV-2010	25790			PLR	3.6/22.9	24.1	
13-DEC-2010	26038					24.2	
Chubut test site							
14-JUL-2010	23821	1.1	SLC	FBD	3.2/14.9	39.0	Ascending
12-AUG-2010	24244						
24-AUG-2010	24419						
18-APR-2011	27876			PLR	3.6/22.9	24.2	
						24.1	

SLC: Single Look Complex.
FBD: Fine Beam Double Polarization (HH, HV). Pixel resolution: 20-m. PLR: Quad polarization (HH, HV, VH, and VV). Pixel resolution: 30-m.

A Digital Elevation Model was used for orthorectification of the ALOS PALSAR images. Sample spacing for the SRTM data set used is 1 arc-second in latitude and longitude (approximately 30-m at the equator), consistent with NGA's existing DTED Level 2 product. This product was distributed by CONAE (Argentina Spatial Agency).

The geodetic reference for SRTM data is the WGS84 EGM96 geoid as documented at http://earth-info.nga.mil/GandG/wgs84/gravitymod/index.htm.

Del Valle, H., Hardtke, L., Blanco, P. y Sione, W. (2013): "Assessment of land degradation Using Shannon entropy Approach On Polsar Images In Patagonian Coastal deserts", GeoFocus (Artículos), nº13-2, p. 84-111. ISSN: 1578-5157

The collection of Landsat (TM/ETM+) orthorectified images available through Global Land Cover Facility (GLCF) at http://glcfapp.glcf.umd.edu:8080/esdi/, and images provided by CONAE (Argentine Space Agency) were used as reference source (table 3). For a proper integration of the thematic information extracted from both datasets, it was crucial for the Landsat and ALOS PALSAR data to be accurately coregistered with each other. The registration accuracy between these data was established with the use of a gradient cross-correlation technique (Campbell & Wu, 2008).

We visited the study area in spring and summer from 2007 to 2010 for the ground truth data collection and validation of results (Blanco *et al.*, 2008; del Valle *et al.*, 2008 and 2010). Field observations include stratified soil sampling and analysis, long term field observations of vegetation and biodiversity in specific sites.

Table 3. LANDSAT datasets

Path-Row	Date
226-088	2005-10-06 (ETM+)
227-088	2005-10-13 (ETM+)
227-089	2010-10-11 (ETM+), 2009-04-07 (TM)
227-090	2009-05-17 (ETM+), 2009-04-07 (TM)
228-088	2010-06-12 (ETM+), 2009-02-25 (TM)
228-089	2011-05-14 (ETM+), 2009-02-09 (TM)
228-090	2009-06-25 (ETM+), 2009-02-25 (TM)

2.3. Polarimetric target analysis

Flow methodology is shown in figure 2. Polarimetric processing involved the use of three, free, open-source software tools: PolSARpro 4.2 (Pottier *et al.*, 2009), MapReady 3.1.22 (Gens & Logan, 2003), and NEST 4C-1.1 (Array Systems Computing, 2012). The first provides a diversity of polarimetric capabilities, while the second performs terrain correction and prepares the PolSARpro products for ingestion into a GIS. The third software was used to replace metadata, colour manipulation, import and export PolSARpro format, export view (png, kmz), perform mosaics, and create mask out the sea.

Images were analyzed individually, and in some cases ALOS PALSAR 20-m orthorectified mosaic product were created from the ascending path using the Fine Beam Dual polarization (FBD) mode. Thus, images were converted to the normalized radar cross section in decibel. The conversion between the amplitude (DN) and the normalized radar cross section (σ^0) is given as follows (Shimada, 2006):

$$\sigma^0 = 10 * \log_{10} [DN^2] + CF$$

where CF = -83.0 dB for both HH and HV polarizations.

Del Valle, H., Hardtke, L., Blanco, P. y Sione, W. (2013): "Assessment of land degradation Using Shannon entropy Approach On Polsar Images In Patagonian Coastal deserts", GeoFocus (Artículos), nº13-2, p. 84-111. ISSN: 1578-5157

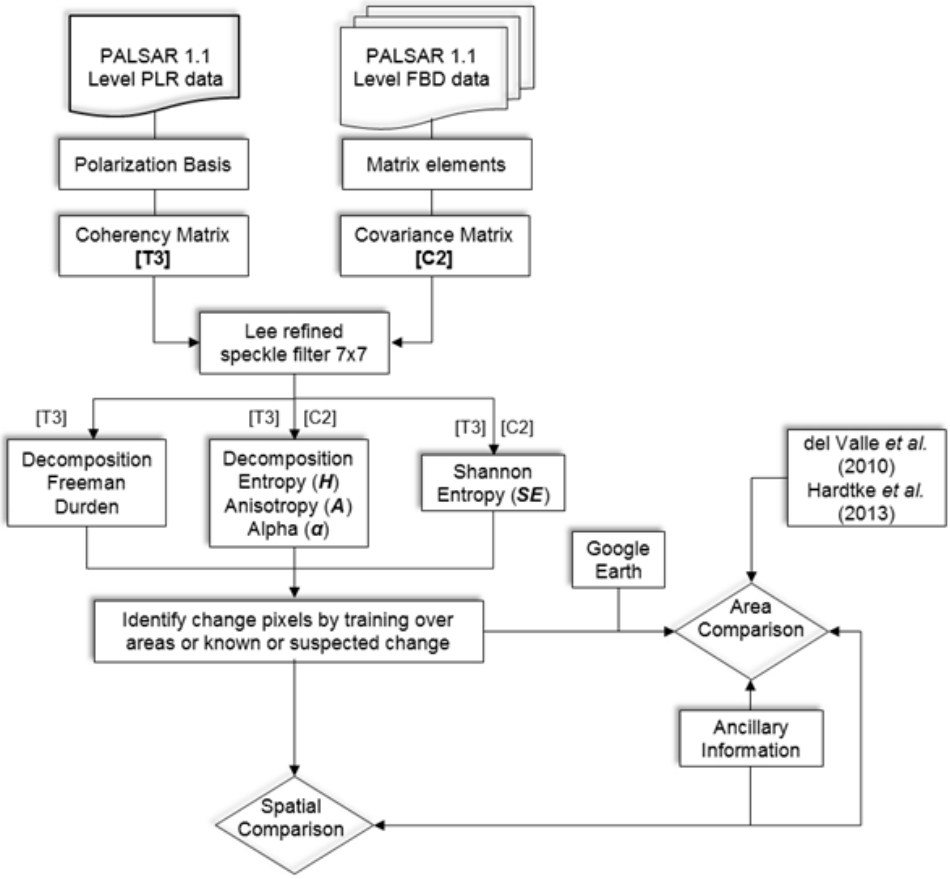

Figure 2. Methodology flowchart. Detecting spectral changes and identifying sources of change.

The procedure of data processing for targets detection mainly contains: polarimetric data calibration, matrix analysis of covariance [*C2*] and coherency [*T3*] matrices, polarimetric basis transform, polarization decomposition and polarimetric parameters computation. The [*T3*] matrix is closely related to the physical and geometric properties of the scattering process, and thus allows better and direct physical interpretation. The [*C2*] matrix is directly related to the system measurable.

The SE_T was computed for [*C2*] and [*T3*] matrices, as a sum of two contributions related to intensity (SE_I) and polarimetry (SE_p):

Del Valle, H., Hardtke, L., Blanco, P. y Sione, W. (2013): "Assessment of land degradation Using Shannon entropy Approach On Polsar Images In Patagonian Coastal deserts", GeoFocus (Artículos), nº13-2, p. 84-111. ISSN: 1578-5157

$$SE_T = SE_I + SE_P$$

$$SE_I = 2 \log \left(\frac{\pi e \, Tr\,[C2]}{2} \right) \qquad SE_P = \log \left(4 \frac{det\,[C2]}{Tr\,[C2]^2} \right)$$

$$SE_I = 3 \log \left(\frac{\pi e \, Tr\,[T3]}{3} \right) \qquad SE_P = \log \left(27 \frac{det\,[T3]}{Tr\,[T3]^3} \right)$$

Where SE_I is the intensity contribution (positive or negative value) that depends on the total backscattered power and SE_P is the polarimetric contribution that depends on the Barakat degree of polarization P_T, so the range of SE_P is $(-\infty,0)$. This term is negative since the degrees of polarization vary between zero and one. Strictly positive values of SE_P correspond to eigenvalues of SE_I that are not equal and thus, in general, to partial correlation between the elements of the scattering matrix. Since partial correlation decreases randomness, it also decreases the entropy, which explains the no positivity of SE_P. Low SE_P value means deterministic scattering mechanism, while high SE_P means random scattering mechanism. For [T3] matrices we calculated the normalized SE_T, SE_I, and SE_P.

We also investigate three popular parameters like entropy (H), Anisotropy (A) and alpha angle (α) in order to provide complementary physical interpretation (Cloude & Pottier, 1997). The H measures the degree of the randomness of the scattering process, for which $H \rightarrow 0$ corresponds to a pure target, whereas $H \rightarrow 1$ means the target is a distributed one. The A gives the relative importance of the second and the third eigenvalues. But it is most meaningfully used while $H > 0.7$. Another important parameter is the angle α which measures the dominant scattering mechanism within a specified neighborhood. The value of α varies between 0 and 90º. Zero degrees represents odd-bounce scattering from flat surfaces. Even-bounce phenomenon can be observed around α = 90º, while α = 45º denotes dipole scattering.

The Freeman-Durden decomposition of polarimetric coherency matrix [*T3*] used is a technique for fitting a physically based, three-component scattering mechanism model (double bounce, canopy layer and rough surface) to the polarimetric SAR observations, without utilizing any ground truth measurements (Lee & Pottier, 2008).

2.4. Validation

The accuracy of the SE_T map was assessed using a set of ground observations based on remotely sensed data that have higher accuracy for the same study area (del Valle *et al.*, 2010; Hardtke *et al.*, 2013).

Del Valle, H., Hardtke, L., Blanco, P. y Sione, W. (2013): "Assessment of land degradation Using Shannon entropy Approach On Polsar Images In Patagonian Coastal deserts", GeoFocus (Artículos), nº13-2, p. 84-111. ISSN: 1578-5157

The error matrix was based on stratified and randomly selected sites, ensuring at least 50 samples per class. In addition, we displayed the resulting SE_T maps in the image windows of the NEST software, which is linked with Google Earth (export view as kmz), and carried out visual evaluation of the classes.

3. Results and discussions

3.1. Río Negro test site

3.1.1. Spectral and backscattering characterization

Figure 3 describes the backscatter values (L-band σ^0_{HH} and σ^0_{HV}) covering a wide range of surface roughness (influenced by terrain features, vegetation physiognomy and cover, and land degradation) and moisture conditions (table 4, Cruzate *et al.*, 2012). The backscattering intensity changes with these parameters and produces image brightness variations, expressed as changes in the pixel color levels of the images (del Valle *et al.*, 2010).

The stabilized dunefields, linear reflections (vegetated dune crests), gullies, cliff scarps, grasses on roads, terrain slopes towards radar, dense vegetation, rough surface, irrigated croplands and man-made objects (urban) can be clearly identified by their bright reflections (very high and high backscatter, red and orange colors). Active sand dunes, calm water, temporary or permanent saltlakes and sand beaches show smooth dry dark surfaces (low backscatter, black color). The interdune space and some paddocks show violet color. The burnt areas (wildfires summer 2001), bare agricultural lands and the sparse vegetation and pebbles covering the dissected gravel plains ("Rodados Patagónicos") produce moderate radar returns and appear as blue and cyan colors, in contrast to sand covered areas (del Valle & Blanco, 2006). The burned and unburned areas seem not to be discriminated remarkably by backscatter in the figure 3 since values for the burnt and unburned classes resume to similar levels. But the backscattering intensity of burnt areas after bushfire clearly increases with that before and after the fire. The reduced volume scattering, bare, dry soil and a decreasing dielectric constant result after wildfire in a low backscatter, in fact the shrublands were severely burned and only left the trunk of the shrubs. Medium level of vegetation, agricultural crops and moderately rough surfaces present moderate backscatter (green and yellow colors).

In general, tone variations of the SAR images are more relevant to spectral or dynamic properties than to surface roughness (Qong, 2000). However, in relation with the aeolian processes, windblown sand easily produces changes in surface roughness and could be the cause of the variations of the backscatter coefficient (Prigent *et al.*, 2005). Sand movement randomly changes the micro-geometry of the sand scatters on the terrain surface. The very dark features of mobile sand over a bright matrix are not only direct evidence of sand mobility, but they also effectively delineate the outlines of active sand dunes and visually indiscernible thin sand sheets (Liu *et al.*, 2001; Stephen & Long, 2004).

Del Valle, H., Hardtke, L., Blanco, P. y Sione, W. (2013): "Assessment of land degradation Using Shannon entropy Approach On Polsar Images In Patagonian Coastal deserts", GeoFocus (Artículos), nº13-2, p. 84-111. ISSN: 1578-5157

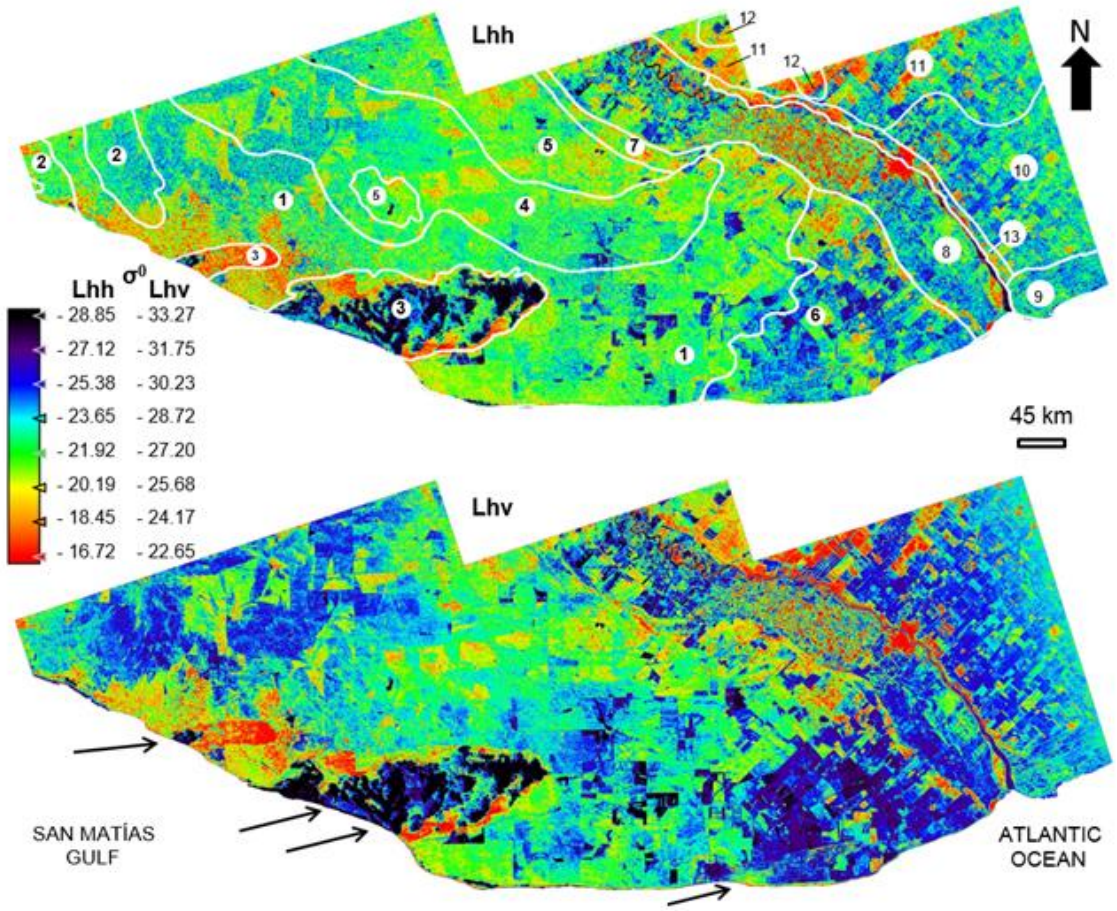

Figure 3. Río Negro test site. 2010 ALOS PALSAR mosaic of 3 Level 1.1 (SLC) fine beams, dual polarimetric scenes acquired 21-July, 19-August and 22-September (L-band σ^0_{HH} and σ^0_{HV}). The southwest wind component (black arrows) overwhelmingly prevails throughout the area. See references in table 4.

Del Valle, H., Hardtke, L., Blanco, P. y Sione, W. (2013): "Assessment of land degradation Using Shannon entropy Approach On Polsar Images In Patagonian Coastal deserts", GeoFocus (Artículos), nº13-2, p. 84-111. ISSN: 1578-5157

Table 4. Limiting soil factors

Unit Fig. 3	Landform	Terrain slope	Soil textural classes		Limiting soil factors in order of importance
			Surficial	Sub-surficial	
1	Gravel plains	Nearly level (0.5 to 2%) and very gentle slopes (2 to 5%)	Sand	Sand	Wind erosion; Shallow soil depth; Low retention of humidity
2					Water erosion; Alkaline <0.50 m depth; Low retention of humidity
3	Active sand dunes (sandhills), stabilized dunefields	Nearly level (0.5 to 2%), very gentle slopes (2 to 5%) and gentle slopes (5 to 9%)			Wind erosion; Low retention of humidity
4	Gravel plains	Nearly level (0.5 to 2%) and very gentle slopes (2 to 5%)	Clay loam	Clay loam	Alkaline <0.50 m depth; Water erosion
5					Alkaline <0.50 m depth; Salt-affected soils; Water erosion
6			Sand	Sand	Wind erosion; Low retention of humidity
7			Loamy sand	Loamy sand	Wind erosion; Water erosion; Alkaline <0.50 m depth
8	Floodplains and terraces	Level (0 to 0.5%) and nearly level (0.5 to 2%)	Clay, clay loam, sandy clay loam, sandy clay, sandy loam		Poor drainage; Alkaline <0.50 m depth; Salt-affected soils
9	Aeolian mantles and sandhills	Nearly level (0.5 to 2%) and very gentle slopes (2 to 5%)	Sand	Sand	Wind erosion; Low retention of humidity
10	Gravel plains		Sandy clay loam	Loam	Wind erosion; Alkaline <0.50 m depth
11			Sandy loam	Sandy loam	Wind erosion
12					
13	Stream beds and river valley	Level (0 to 0.5%) and nearly level (0.5 to 2%)			Poor drainage; Salt-affected soils

Source: Cruzate *et al.* (2012).

Del Valle, H., Hardtke, L., Blanco, P. y Sione, W. (2013): "Assessment of land degradation Using Shannon entropy Approach On Polsar Images In Patagonian Coastal deserts", GeoFocus (Artículos), nº13-2, p. 84-111. ISSN: 1578-5157

3.1.2. Burned and unburned areas: Interpretation of polarimetric parameters

Figure 4A-D presents a subset showing an old burned area (wildfire summer 2001) with small new burnings (2004-2005). The burned and unburned areas can be appreciated clearly in the Landsat image (fig. 4A).

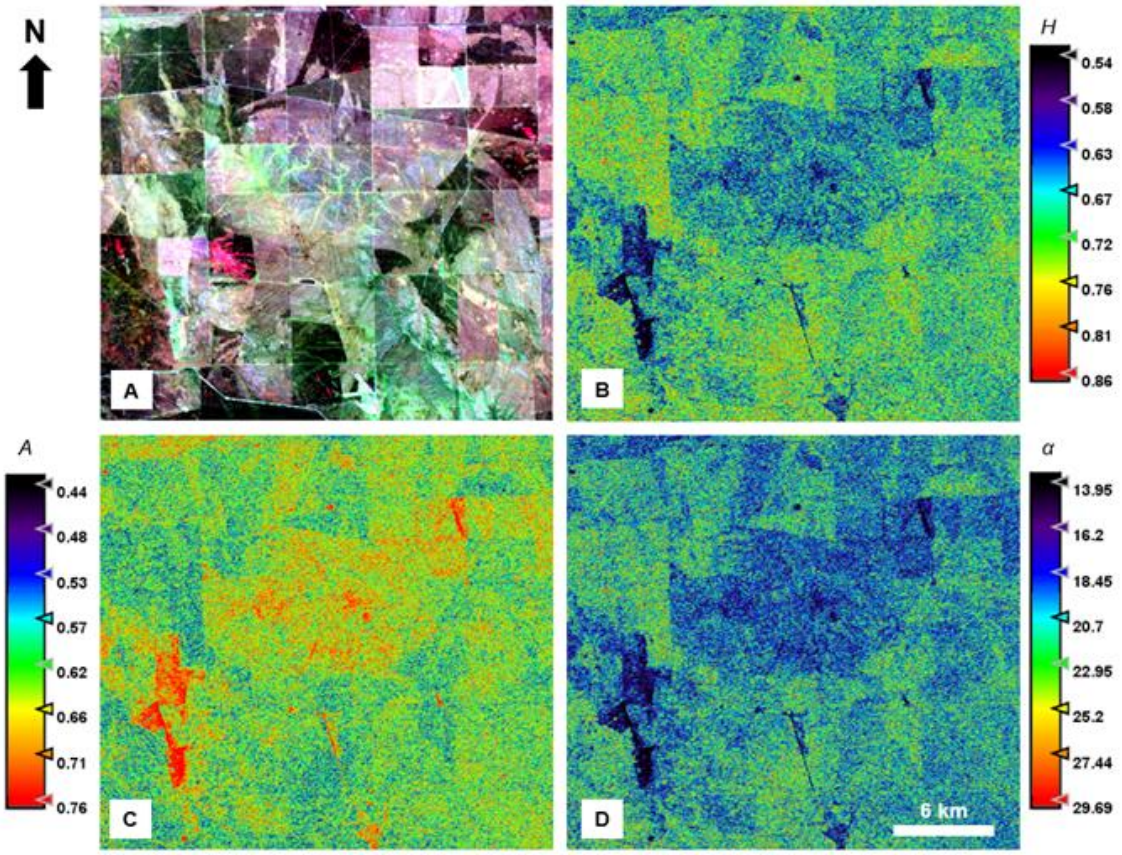

Figure 4A-D. Río Negro test site. Subset showing an old burnt area (wildfire summer 2001) with small new burnings (2004-2005). 4A. Landsat ETM+ RGB 742 on October 13, 2005, showing fire scars (blotchy red areas) and the location of the old burned (light tones) and unburned (dark tones) areas. 4B. Entropy (*H*). 4C. Anisotropy (*A*). 4D. Alpha angle (*α*).

Figures 4B-D shows the *H*, *A*, and *α* parameters affected by noise. However, it has been shown that decreasing *H* is related to higher degradation level (fig. 4B). Burned areas have a medium value of *H*, indicating dominance of a surface scattering. From a practical point of view, the *A* can be employed as a source of discrimination only when *H* >0.7. The reason is that for lower entropies, the second and third eigenvalues are highly affected by noise. But in our case it can be observed that the three parameters present noise. In the figure 4B-C it can be clearly observed the way anisotropy discriminates different configurations presenting almost the same value of entropy. Results of the Cloude-Pottier decomposition represented in *H-α* feature space are shown in figure 5 (low vegetation, zone 6). This zone reveals the increase in entropy due probably to: (*i*) changes in

Del Valle, H., Hardtke, L., Blanco, P. y Sione, W. (2013): "Assessment of land degradation Using Shannon entropy Approach On Polsar Images In Patagonian Coastal deserts", GeoFocus (Artículos), nº13-2, p. 84-111. ISSN: 1578-5157

surface roughness and (*ii*) canopy propagation effects (regeneration of the vegetation?). Some points in *H-α* feature space of burned and unburned areas were inside a non-feasible region.

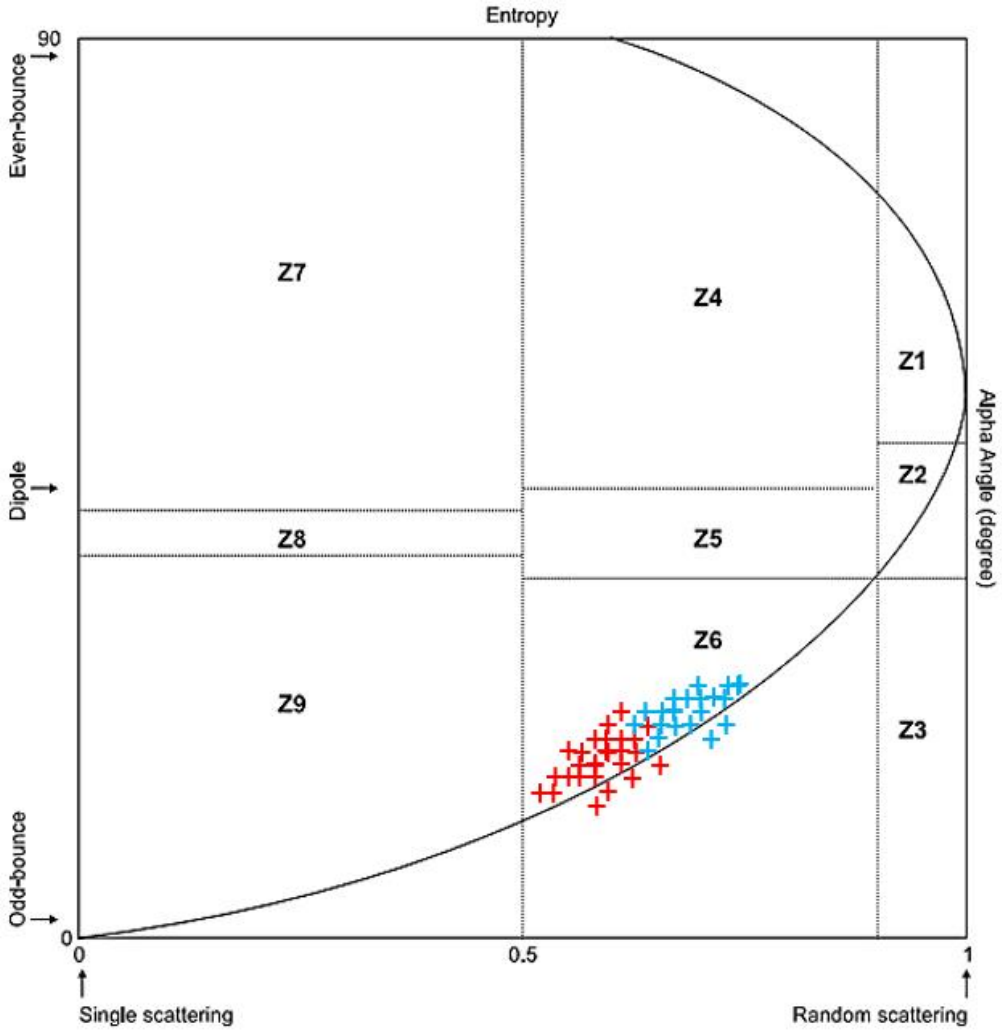

Figure 5. Segmentation of entropy-alpha feature space (modified from Cloude & Pottier, 1997). Zone 6 (Z6) corresponds to medium entropy surface scattering (low vegetation). Burned areas (red cross), unburned areas (blue cross).

Figure 6A-C shows the two different contributions to the *SE* estimated by spatial averaging from a partition in statistically homogeneous regions. Burned and unburned areas features can be comparatively clearer. SE_T is the sum of SE_I and SE_P that contains not only intensity information, but also polarization data. The burned areas show moderate to low SE_T values (-6.0 to -7.4) and its equivalent with the Span *dB* values (-18.5 to -21.3), while the unburned areas are represented by moderate to high SE_T values (-6.1 to -4.3) and with the Span *dB* values (-18.51 to -14.8). These results conserve more the texture and show clearer patterns recognition**,** what is a help to detect and

Del Valle, H., Hardtke, L., Blanco, P. y Sione, W. (2013): "Assessment of land degradation Using Shannon entropy Approach On Polsar Images In Patagonian Coastal deserts", GeoFocus (Artículos), nº13-2, p. 84-111. ISSN: 1578-5157

assess the types of targets. The burned areas have low polarimetric and intensity contributions to *SE* because of high degrees of polarization and a weak total backscattered power. Figure 6D shows the span values in decibels (sum of eigenvalues) that it coincides texturally with SE_T.

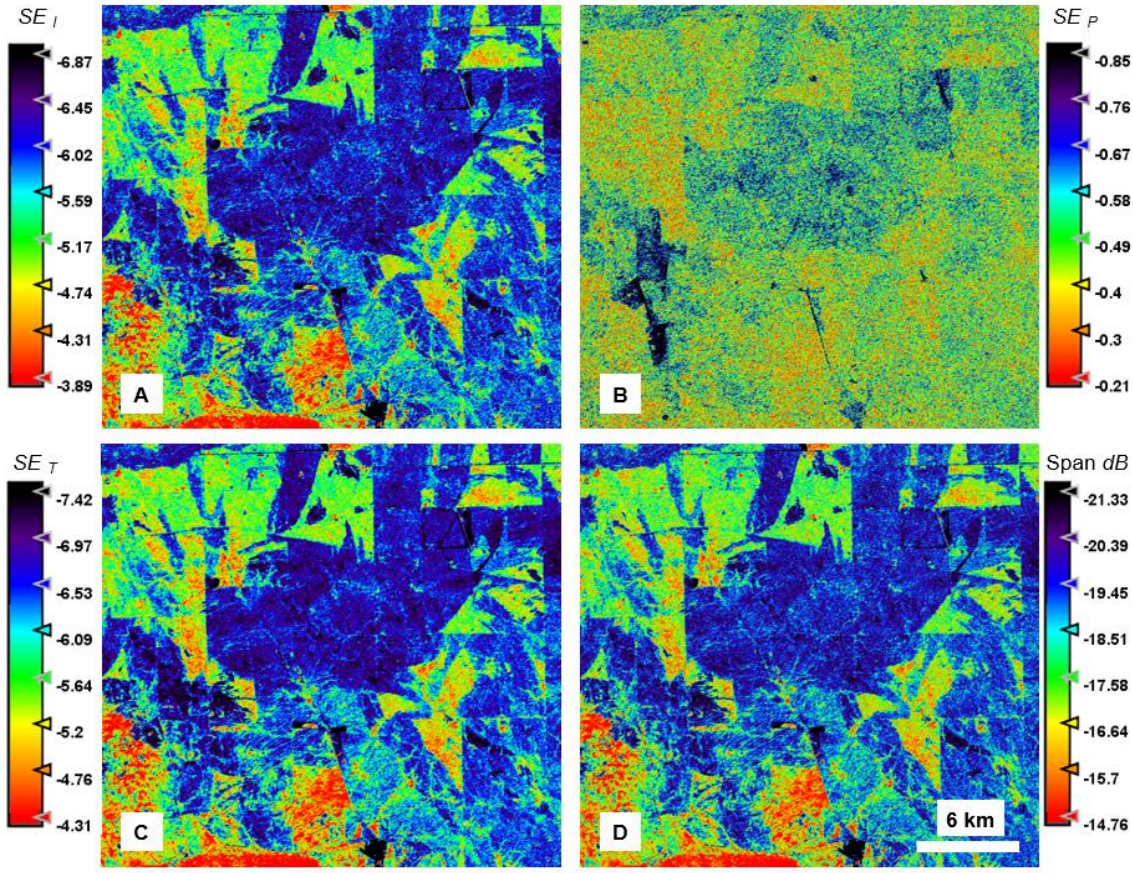

Figure 6A-D. Río Negro test site. 6A. Shannon Entropy Intensity (SE_I). 6B. Shannon Entropy Polarimetry (SE_P). 6C. Shannon Entropy Total (SE_T). 6D. Span (*dB*). Note the differences with figure 4A-D.

3.1.3. Wind-driven land degradation processes

Wind erosion in the eastern Río Negro test site produces strong signals of environmental changes leading to desertification in the form of deflating surfaces, dust storms, and migrating sand dunes. Two critical factors that influence the severity of wind erosion are the percent of vegetation cover and the type of terrain surface. Short-term variation in wind erosion is controlled by factors such as high interannual rainfall variability, droughts, localized wildfires, and livestock grazing (Blanco *et al.*, 2008).

Del Valle, H., Hardtke, L., Blanco, P. y Sione, W. (2013): "Assessment of land degradation Using Shannon entropy Approach On Polsar Images In Patagonian Coastal deserts", GeoFocus (Artículos), nº13-2, p. 84-111. ISSN: 1578-5157

The boundaries of the sand dune megapatches are sharp although not fully stable, as illustrated in figure 7A. This figure also shows a set of "plumes" of flow extending downwind of the paddocks. These plumes may be the result of sand- blasting of the native desert plants caused by the increased wind erosion. There are some wind-related features that provide clues to the wind direction (Schaber, 1999). We can find from figure 7B that SE_T can discriminate the aeolian processes properly, all of this is done in one calculation. The high values (red color, >-4.68) of SE_T correspond mostly to psammophytic species (mainly the natives *Hyalis argentea* and *Sporobolus rigens*) that recolonize**s** the dunes. Thin red-orange lines (-4.68/-5.38) are bright reflections from steep sand ridge crests. The sand ridges, now smoothed and partially reworked, seem to have derived from a mixture of active and inactive barchanoid ridges and parabolic dunes (del Valle *et al.*, 2010). The active sand dunes in megapatches are distinctively darker (black and violet colors, -9.55 and -8.86). The cyan (-7.46) and blue (-8.16) colors represent a severe status of land degradation (overgrazing and old burned areas). The stabilized discontinuous aeolian mantles are represented by yellow color (-6.07)**,** with grasses and scrubs shown in red and orange colors. The green color (-6.77) shows a contrast in land management (fence line) with moderate grazed condition.

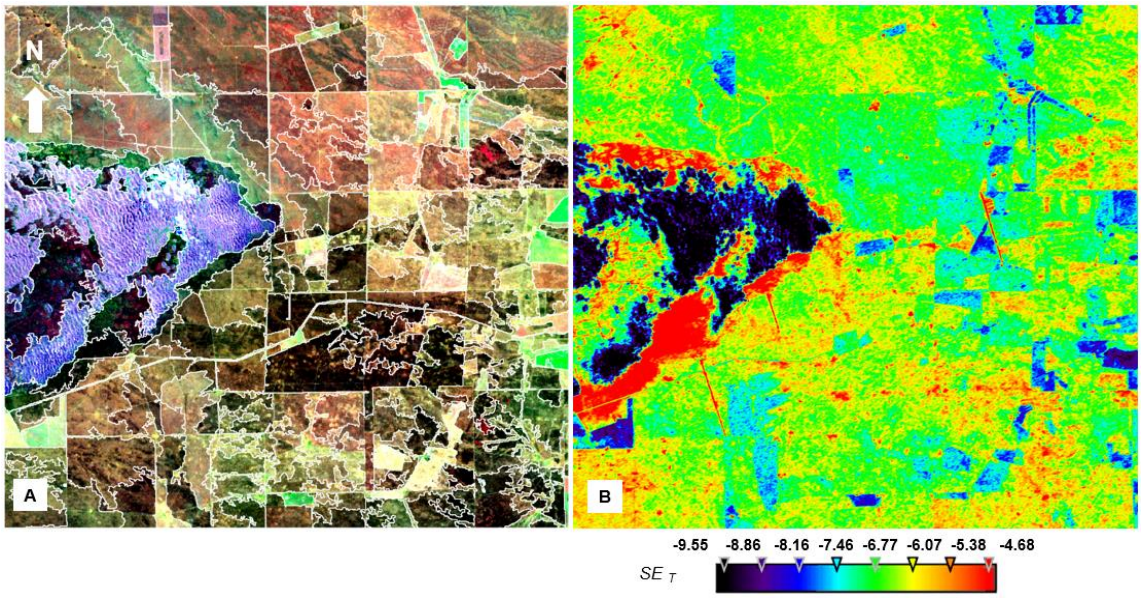

Figure 7A-B. Río Negro test site. Subset showing the active sand dune megapatches front in pasturelands. 7A. Segmentation and classification Landsat ETM+ RGB 742 on October 13, 2005 (unpublished del Valle *et al.*). The image include objects on a complex background (changes caused by natural disturbances and grazing-induced desertification). 7B. Shannon Entropy Total (SE_T) contribution. This parameter preserves the details, highlights edges, and decreases random noise.

Del Valle, H., Hardtke, L., Blanco, P. y Sione, W. (2013): "Assessment of land degradation Using Shannon entropy Approach On Polsar Images In Patagonian Coastal deserts", GeoFocus (Artículos), nº13-2, p. 84-111. ISSN: 1578-5157

3.1.4. Land-use/land-cover relationships

Figure 8A-B presents the SE_T and three contributions of each scattering mechanism. Freeman-Durden decomposition shows that rough surface contribution describes texture characteristic more clearly than other contributions. According to the actual situation in the study area and penetration for L-band, multiple scattering can occurs in subsurface medium (such as arid-semiarid saline medium), with volume (canopy layer) scattering and surface scattering interaction. *SE*, as shown in figure 8A, conserves more details that probably express the features also of subsurface targets.

The Freeman-Durden algorithm has been widely used because of its simplicity and stability, but it has some limitations. As pointed out by Van Zyl *et al.* (2011), a major limitation is that the volume scattering terms all assume the scattering reflection symmetry for the observations. Thus, the decomposition may result in many pixels with a negative power.

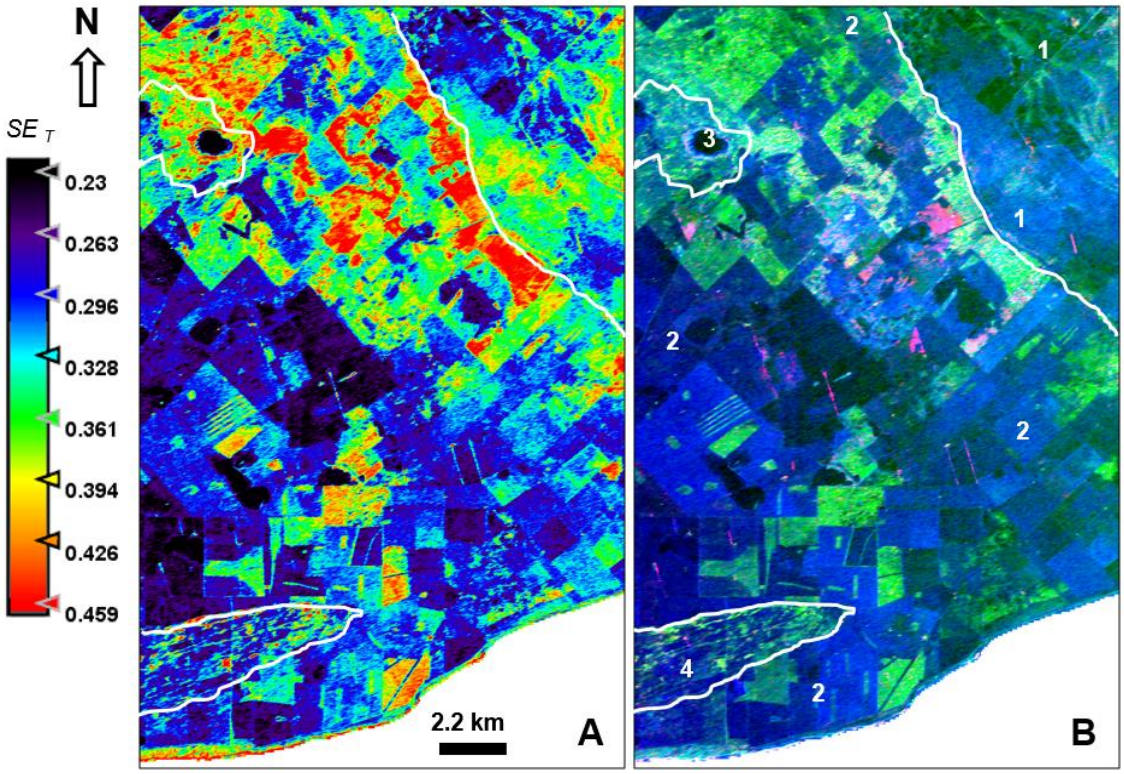

Figure 8A-B. Río Negro test site. Subset showing different land degradation status. Coherency Matrix [T3]. 8A. Normalized Shannon Entropy (SE_T). 8B. Freeman-Durden decomposition (RGB): Double Bounce, Canopy Layer, Rough Surface. 1. Floodplains and terraces. 2. Gravel plains. 3. Depression. 4. Stabilized longitudinal sand dunes with blowouts.

Del Valle, H., Hardtke, L., Blanco, P. y Sione, W. (2013): "Assessment of land degradation Using Shannon entropy Approach On Polsar Images In Patagonian Coastal deserts", GeoFocus (Artículos), nº13-2, p. 84-111. ISSN: 1578-5157

3.2. Northeastern Chubut test site

3.2.1. Valdés Peninsula: Interpretation of polarimetric parameters

The three parameters (*H, A, α*), even though they present moderate noise, have different behavior than in the previous test site (Río Negro). Figure 9A-C shows the three parameters calculated from the L-band data. The so called mean alpha angle attaches an averaged scattering event to each resolution cell by adopting values between 10° and 31°. Low values correspond to surface scattering whereas mean values indicate volume scattering and high values stand for double bounce scattering. The two other parameters – entropy and anisotropy – describe the diversity of the scattering mechanism. In all cases, the rangeland areas show significant randomness, as well as the aeolian areas (south of Valdés peninsula). The variations are consistent with the amount of vegetation present on a field scale. However the results obtained with the SE_T are excellent (figure 10A-C) since they clearly indicate spatial concentration or dispersion, where showing up the orientation and configuration of spatial patterns (see details in figure 10B-C). Stabilized sand deposits are distinctly observed, with defined edges but also signals of ongoing wind erosion. One of the most conspicuous features corresponds to old track sand dunes, a mixture of active and inactive barchanoid ridges and parabolic dunes. This is a clear example of deactivation of migrating dunes under the influence of vegetation (del Valle *et al.*, 2008 and 2010).

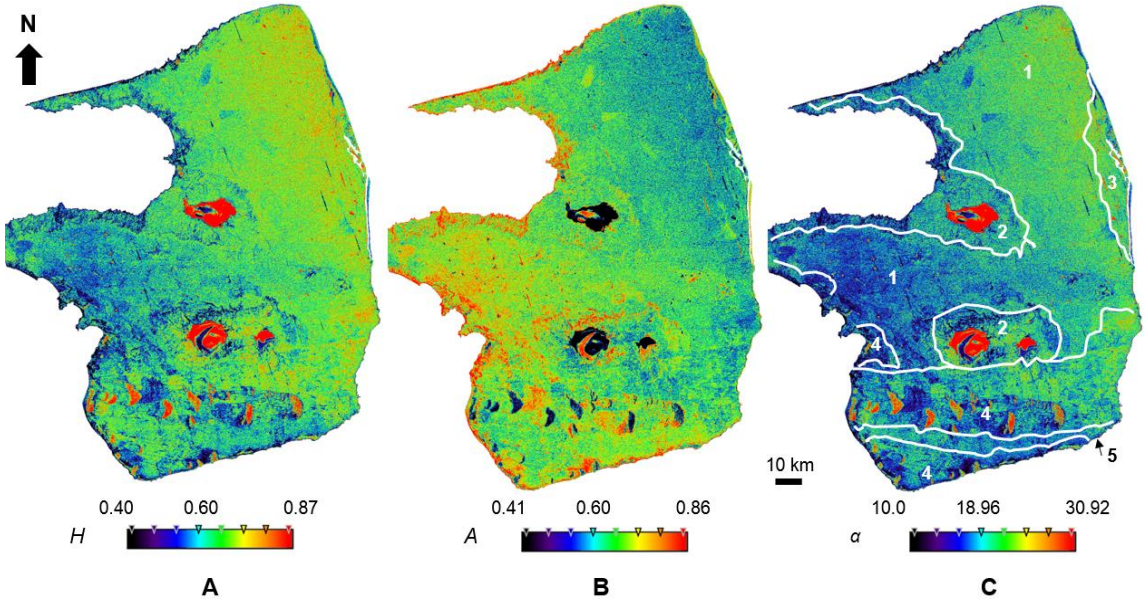

Figure 9A-C. Chubut test site (Valdes Peninsula). 9A. Entropy (*H*). 9B. Anisotropy (*A*). 9C. Alpha angle (*α*). 1. Gravel plains. 2. Cliffs, scarps and tectonic depressions with saltlakes. 3. Valdes Creek. 4. Dunefields. 5. Gravel plain with discontinuous aeolian mantles.

Del Valle, H., Hardtke, L., Blanco, P. y Sione, W. (2013): "Assessment of land degradation Using Shannon entropy Approach On Polsar Images In Patagonian Coastal deserts", GeoFocus (Artículos), nº13-2, p. 84-111. ISSN: 1578-5157

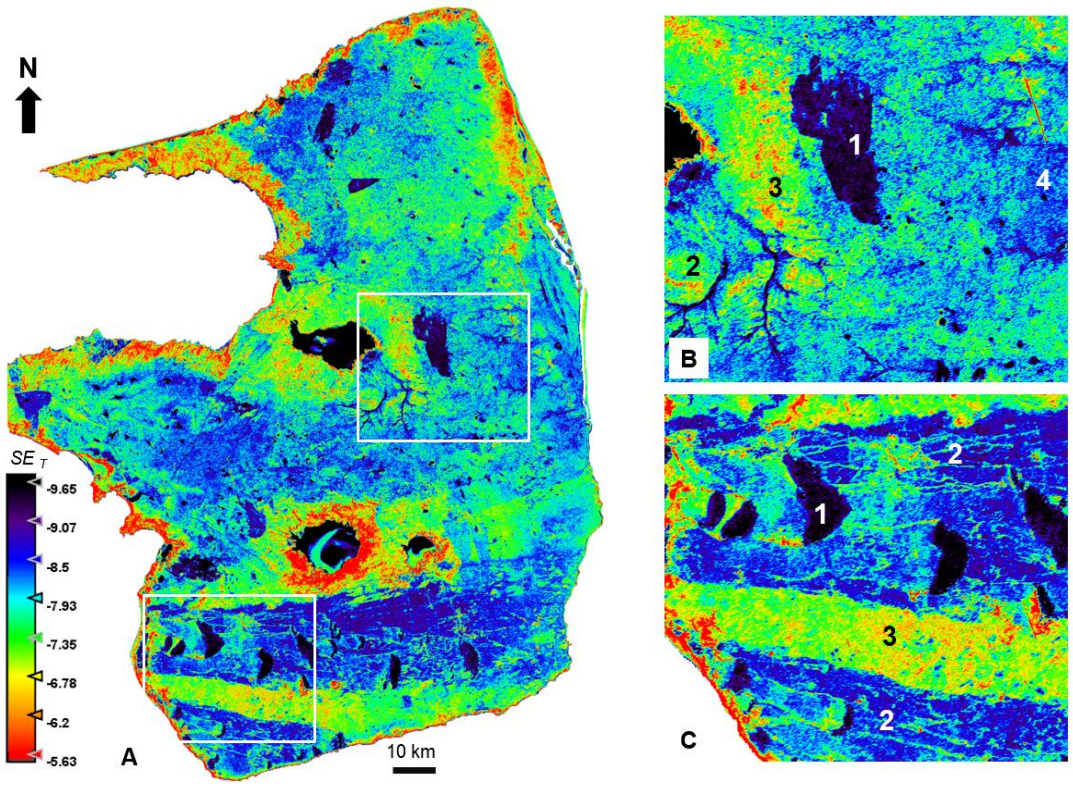

Figure 10A-C. Chubut test site (Valdes Peninsula). Shannon Entropy Total (SE_T). 10A. Valdes Peninsula. 10B. 1. Old burnt area. 2. Water erosion (gullies, rills). 3. Aeolian mantles stabilized (shrub with grass steppe). 4. Overgrazing. 10C. 1. Active sand dune megapatches (colony of sand dunes). 2. Old track of sand dunes stabilized. 3. Aeolian mantles discontinuous stabilized on gravel plains.

3.2.2. Burned and unburned areas: Madryn city surroundings

Figure 11 shows an example of burned areas with details in the SE_T analysis of SAR imagery allowing to discriminate the burnt areas from the rangelands areas and, consequently, detecting the burnt scars. The changes in SE_T seem to be associated to the roughness and moisture conditions of the recent and old burned areas, i.e., becoming detectable when there is an increase in roughness and moisture content in the soil. This behavior is similar to that of burned areas in Rio Negro test site. Low values of SE_T (-7) represent the burned area in the graphs (transect profile plot). The SE_T contribution compensate for local changes (without confusing) and denoises the output.

Del Valle, H., Hardtke, L., Blanco, P. y Sione, W. (2013): "Assessment of land degradation Using Shannon entropy Approach On Polsar Images In Patagonian Coastal deserts", GeoFocus (Artículos), nº13-2, p. 84-111. ISSN: 1578-5157

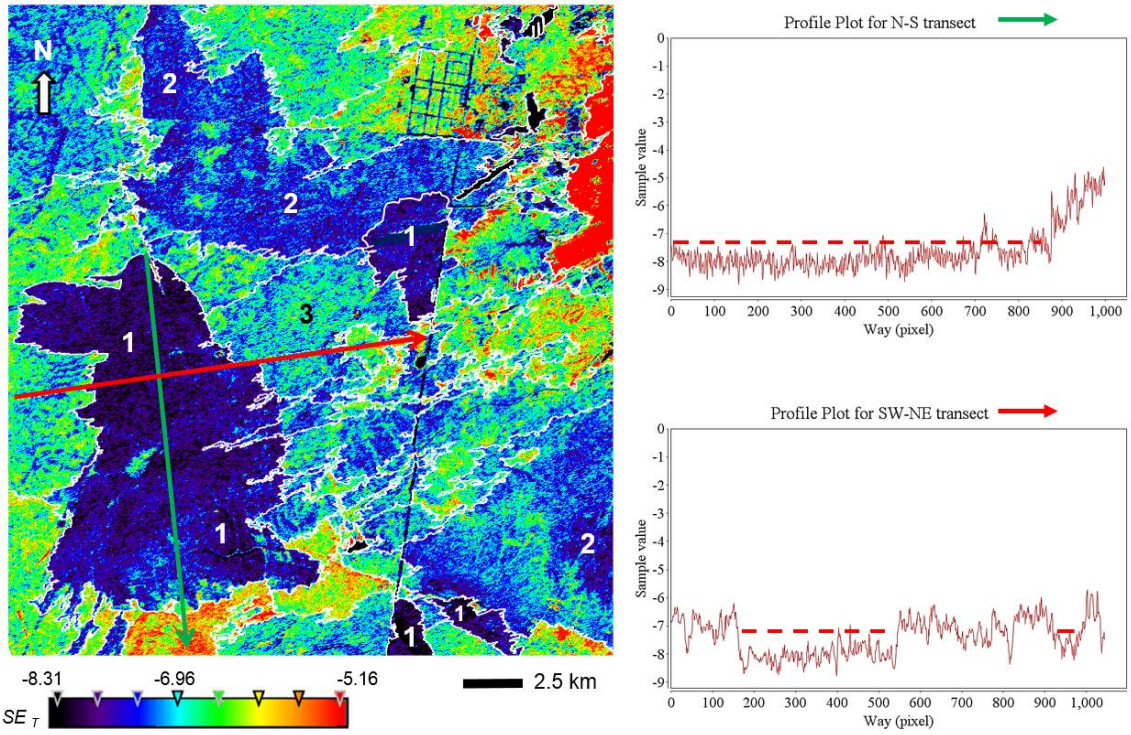

Figure 11. Chubut test site (Madryn city surroundings). Recent and old burn scars (1, and 2-3, respectively). Plots for Shannon Entropy Total (*SE T*). The dashed red line represent the burned areas.

3.2.3. Rough surface versus volume scattering

Figure 12A-B shows a comparison between the *SE T* and the Freeman-Durden decomposition. Rough surface scattering by non-vegetated surface or low vegetation (<40%, 40-60% vegetation cover) can cause significant depolarization and produces high cross-polar levels that can appear as volume scattering in the Freeman and Durden decomposition (see figure 12B, 1, 2). Consequently, a rough surface may be classified as a volume class, and then could be misinterpreted as vegetation. Lee *et al.* (2004) observed this behavior at higher radar frequencies (X and C-bands), but not for the L-band. In summary, like many other decomposition techniques, Freeman and Durden decomposition has some limitations. Some of the misinterpretation may be avoided with *SE T*. However, problems associated with inherent PolSAR scattering characteristics would remain. The terrain type identification has to be carefully interpreted.

Del Valle, H., Hardtke, L., Blanco, P. y Sione, W. (2013): "Assessment of land degradation Using Shannon entropy Approach On Polsar Images In Patagonian Coastal deserts", GeoFocus (Artículos), nº13-2, p. 84-111. ISSN: 1578-5157

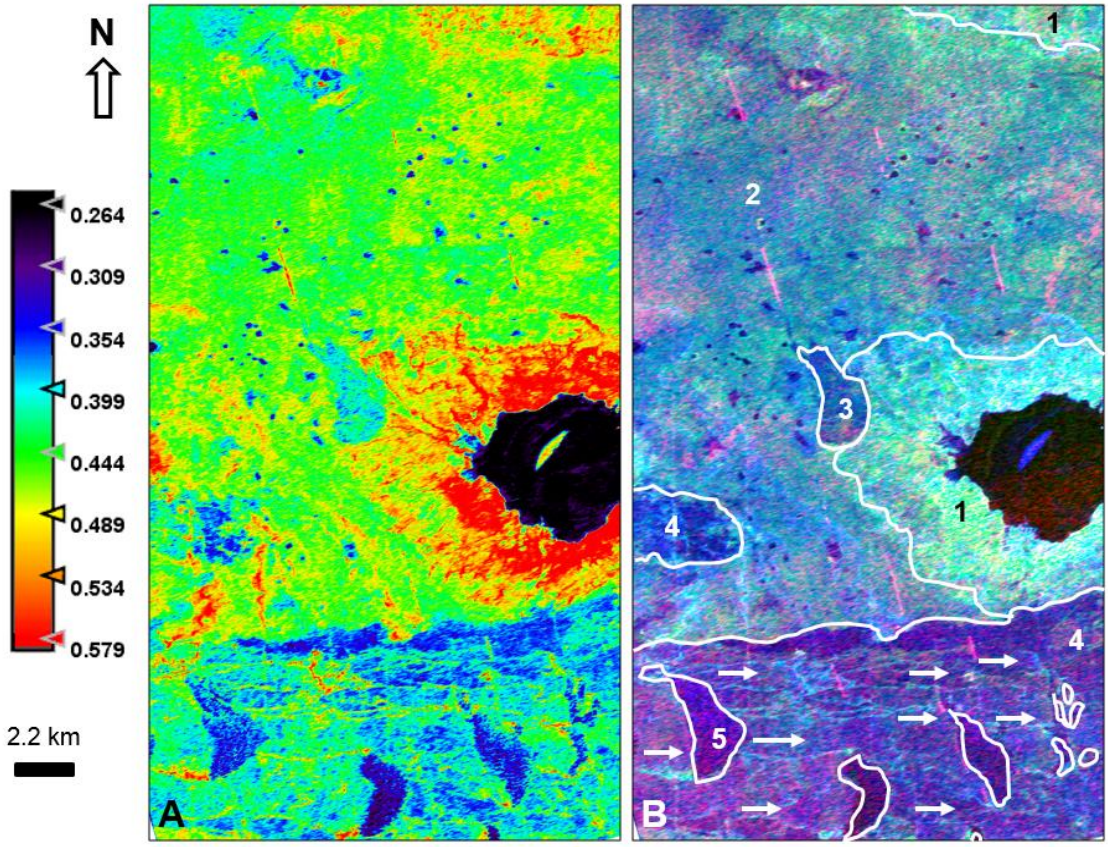

Figure 12A-B. Chubut test site (Valdes peninsula). Subset showing different land degradation status. Coherency Matrix [T3]. 12A. Normalized Shannon Entropy (SE_T). 12B. Freeman-Durden decomposition (RGB): Double Bounce, Canopy Layer, Rough Surface. 1. Tectonic depressions with saltlake. Gully erosion in the scarp areas. 2. Gravel plains (overgrazed areas). 3. Burned area. 4. Stabilized dunefields. 5. Active sand dune megapatches (colony of sand dunes). The white arrows indicate the old tracks sand dune.

3.3. Validation

The detectability and accurate characterization of natural disturbances and human impacts using remotely sensed data are influenced by the type of disturbance, the magnitude and duration of the modified signal, and natural variability (species/stand/landscape). These factors can often result in high errors of omission and commission. However, the mapping and measurements of local scale changes requires levels of accuracy in mapping which are possible to reach with SAR data.

Table 5 summarizes the accuracy assessment from SE_T –based land cover classes. The classification accuracy obtained with the different classes present an overall accuracy (84.1%) and a higher KHAT statistic value (83.3%).

Del Valle, H., Hardtke, L., Blanco, P. y Sione, W. (2013): "Assessment of land degradation Using Shannon entropy Approach On Polsar Images In Patagonian Coastal deserts", GeoFocus (Artículos), nº13-2, p. 84-111. ISSN: 1578-5157

Table 5. Accuracy assessment from SE_T -based land cover classes

Land cover	Percentage				
	UA	**PA**	**EO**	**EC**	**K**
Recent burn scar	86.5	85.2	20.0	26.4	90.1
Old burn scar	75.5	74.1	25.9	29.5	81.3
Active sand dunes	81.9	85.9	24.1	28.1	86.2
Stabilized dunefields with deflation areas	79.6	73.9	20.4	22.5	79.9
Aeolian mantles (sand sheets) discontinuous, stabilized on gravel plains	77.1	70.2	29.8	28.9	80.0
Old tracks sand dune	78.1	82.5	27.5	32.6	82.1
Water erosion (gullies, rills)	81.2	84.3	22.7	25.8	84.7
Overgrazed areas	85.7	76.8	20.3	26.0	82.4

- Overall accuracy (%): 84.1
- KHAT statistic (%): 83.3

UA: user´s accuracy. PA: producer´s accuracy. EO: errors of omission. EC: errors of commission. K: Kappa statistic.

The commission errors were lightly predominant. Recent burn scars were confused with asphalt roads, saltlakes and deep, clear water bodies. Problems of signature separability typically bias severe or high damage/impact disturbance categories, resulting to be an overclassification. The presence of other disturbance types (current or past) it could be another source of commission errors. To mitigate commission errors in land degradation mapping, GIS data can be used to create spatial masks of the landscape features most often confused with the land degradation type of interest.

4. Conclusions and future works

The results of *SE* satisfy the description of targets scattering and provides the same conclusions as ground truth observations. It is a feasible way to utilize *SE* to detect disturbance targets and to extract land degradation characteristics. *SE* of the study sites confirms that land degradation is highly dispersed as the entropy. It indicates that the rate of land degradation is quite high and needs proper management to attain land sustainable development. Hence it is imperative that with reliable data, planning and managements should be monitored and managed in a sustainable way to protect the ecosystems.

Even so, entropy only quantifies degrees of disorder in a system that could be insufficient to capture all unique aspects of an evolving land degradation pattern. However, it might be that an analytical description spatial temporal of the *SE* could not be achieved accurately if expert knowledge is lacking. Thus, some kind of interactive approach could be a recommendable way for

Del Valle, H., Hardtke, L., Blanco, P. y Sione, W. (2013): "Assessment of land degradation Using Shannon entropy Approach On Polsar Images In Patagonian Coastal deserts", GeoFocus (Artículos), nº13-2, p. 84-111. ISSN: 1578-5157

integrating, investigating, and updating our understanding about the Patagonian coastal desert within a consistent framework.

Further rule base refinement will allow to map the land degradation status found by segmentation and classification to real land cover classes with distinct bio-physical parameters. Thus, using the object based image analysis on *SE* can be appropriately assigned to the scattering classes and uncertainties can be determined by geometric and context object features. Another future work will include the inclusion of other SAR spaceborne like COSMO-SkyMed (X-band) or Argentine airborne SAR like SARAT (L-band) to increase the information content and temporal coverage.

Acknowledgement

We gratefully acknowledge many helpful comments and suggestions that we have received from anonymous reviewers. This research was carried out within the framework of the forthcoming SAOCOM (**SA**télite **A**rgentino de **O**bservación **CO**n **M**icroondas, Spanish for Argentine Microwaves Observation Satellite) mission, supported by the National Commission on Space Activities (CONAE) jointly with the Department of Science, Technology and Productive Innovation (MINCyT) from Argentina. The SAOCOM project was established for the definition and development of L-band SAR products oriented towards applications for risk and emergency management. The authors would like to thank the above-named organizations for their financial and administrative support.

References

Array Systems Computing (2012): NEST ESA 4C-1.1 software. http://nest.array.ca/web/nest/release-4C-1.1

Ayesa, J.A., López, C.R., Bran, D.E., Umaña, F.J., Lagorio, P.A. (2002): *Cartografía biofísica de la Patagonia Norte.* Relevamiento integrado Nª 76. Instituto Nacional de Tecnología Agropecuaria (INTA), Estación Experimental Bariloche, Argentina.

Barrett, E., Hamilton, M. (1986): *"*Potentialities and problems of satellite remote sensing with special reference to arid and semiarid regions*", Journal of Climatic Change*, 9(1-2), pp. 167-186.

Barros, V. (1986): *Atlas del potencial eólico del sur Argentino.* Centro regional de Energía Eólica (CREE), Chubut, Argentina.

Barros, V., Rivero, M. (1982): *Mapas de probabilidad de precipitación en la Provincia de Chubut.* Contribución no. 54. CENPAT (CONICET), Puerto Madryn, Chubut, Argentina.

Bian, X., Shao, Y., Gong, H., Zhang F., Xie, Ch. (2011): "*Subsurface targets detection with Shannon entropy"*, IGARSS 2011, pp. 1107-1110.

Blanco, P.D., Rostagno, C.M., del Valle, H.F., Beeskow, A.M., Wiegand, T. (2008): *"*Grazing impacts in vegetated dunefields: Predictions from spatial pattern analysis*"*, *Rangeland Ecology Management*, 61, pp. 194–203.

Blumberg, D.G. (2006): *"*Analysis of large aeolian (wind-blown) bedforms using the Shuttle Radar Topography Mission (SRTM) digital elevation data*"*, *Remote Sensing of Environment*, 100, pp. 179-189.

Campbell, N., Wu, X. (2008): "Gradient cross correlation for sub-pixel matching", in *Congress of the International Society for Photogrammetry and Remote Sensing*, Beijing, China, Jul. 2008, 7, pp. 1065–1070.

Cloude, S.R., Pottier, E. (1997): "An entropy based classification scheme for land applications of polarimetric SAR", *IEEE Transactions on Geoscience and Remote Sensing*, 35(1), pp. 68-78.

Cohen, W.B., Goward, S.N. (2004): "Landsat's role in ecological applications of remote sensing", *Bioscience*, 54, pp. 535–545.

Coronato, F. (1992): *"*Influence of the eastern central Patagonia plateaus on the oceanic characteristics of the area climate*"*, *Anales del Instituto de la Patagonia*, 21, pp. 131-146.

Cruzate, G., Gómez, L., Pizarro, M.J., Mercuri, P., Banchero, S. (2012): *"Suelos de la República Argentina 1:500000 y 1:1000000".* Versión Digital Corregida, Revisada y Aumentada (Versión 9.0). SAGyP - INTA - Proyecto PNUD ARG/85/019. http://geointa.inta.gov.ar/node/28

del Valle, H.F., Blanco, P.D., Metternicht, G.I., Zinck, J.A. (2010): *"*Radar Remote Sensing of wind-driven land degradation processes in northeastern Patagonia*"*, *Journal of Environmental Quality*, 39, pp. 62-75.

del Valle, H.F., Rostagno, C.M, Coronato, F.R., Bouza, P.J., Blanco, P.D. (2008): *"*Sand dune activity in north-eastern Patagonia*"*, *Journal of Arid Environments, 7*2, pp. 411-422.

del Valle, H.F., Blanco, P.D. (2006): "Indicadores espectrales del rango de las microondas para la evaluación y monitoreo de la erosión eólica", in E.M. Abraham & G. Beekman (Eds.): *Indicadores de la desertificación para América del Sur, Recopilación y armonización de indicadores y puntos de referencia de la desertificación a ser utilizados en el programa: Combate a la desertificación y mitigación de los efectos de la sequía en América del Sur*. IICA-BID ATN JF 7905-RG. Instituto Interamericano de Cooperación para la Agricultura, Mendoza, Argentina, pp. 65–84.

del Valle, H.F., Rostagno, C.M., Bouza, P.J. (2000): "Los médanos del sur de Península Valdés: Su dinámica y los cambios asociados en los suelos y en la vegetación" (Comisión V, versión CD ROM, 6 pages in pdf format). *XVII Congreso Argentino de la Ciencia del Suelo*.11–14 Apr. 2000. Asociación Argentina de la Ciencia del Suelo, Mar del Plata (Bs. As.), Argentina.

Gens, R., Logan, T. (2003): *Alaska Satellite Facility Software Tools: Manual*. Geophys. Inst. Univ. of Alaska, Fairbanks, AK.

González Díaz, E., Malagnino, C. (1984): *Geomorfología de la provincia de Río Negro.* IX Congreso Geológico Argentino. S.C. de Bariloche, Río Negro, Argentina.

Del Valle, H., Hardtke, L., Blanco, P. y Sione, W. (2013): "Assessment of land degradation Using Shannon entropy Approach On Polsar Images In Patagonian Coastal deserts", GeoFocus (Artículos), nº13-2, p. 84-111. ISSN: 1578-5157

Greeley, R., Blumberg, D.G., McHone, J.F., Dobrovolskis, A., Iversen, J.D., Lancaster, N., Rasmussen, K.R., Wall, S.D., White, B.R. (1997): *"*Applications of space borne radar laboratory data to the study of aeolian processes*", J. Geophys. Res.,* 102, pp. 10971–10983.

Haller, M.J., Monti, A.J., Meister, C.M. (2000): Hoja Geológica 4363-I: Península Valdés, Provincia de Chubut. Programa Nacional de Cartas Geológicas de la República Argentina, 1:250.000. Boletín no. 266. Servicio Geológico Minero Argentino, Buenos Aires, Argentina.

Hansen, M., DeFries, R.S., Townshend, J.R.G., Carroll, M., Dimiceli, C., Sohlberg, R.A. (2003): "Global Percent Tree Cover at a Spatial Resolution of 500 meters: First Results of the MODIS Vegetation Continuous Fields Algorithm*", Earth Interactions*, 7, pp. 1-15.

Hardtke, L.A., del Valle, H.F., Blanco, P.D., Sione, W.F. (2013): "Series temporales de áreas quemadas en regiones semiáridas (2001-2011): Validación de productos globales existentes y propuesta metodológica", *XVI Brazilian Remote Sensing Symposium. Forest Analysis, Deforestation and Burning.* Foz do Iguazu, Brasil, 13-18 Abril, pp. 6308-6315.

Hugenholtz, Ch., Levin, N., Barchyn, T.E., Baddock, M.C. (2012): "Remote sensing and spatial analysis of aeolian sand dunes: A review and outlook", *Earth-Science Reviews*, 111, pp. 319–334.

Le Houérou, H.N. (2005): *The isoclimatic Mediterranean biomes: bioclimatology, diversity and phytogeography*. Cloudley-Thompson JL, préf. 2 vol. Montpellier, copymania.

Lee, J.S., Grunes, M.R., Pottier, E., Ferro-Famil, L. (2004): "Unsupervised Terrain Classification Preserving Polarimetric Scattering Characteristics", *IEEE Transactions on GeoScience and Remote Sensing*, 42, pp. 722-731.

Lee, J.S., Pottier, E. (2008): *Polarimetric Radar Imaging from Basics to Applications*. CRC Press, U.S.

Liu, J.G., Black, A., Lee, H., Hanaizumi, H., Moore, J.M. (2001): "Land surface change detection in a desert area in Algeria using multi-temporal ERS SAR coherence images", *International Journal of Remote Sensing*, 22, pp. 2463-2477.

Morio, J., Réfrégier, P., Goudail, F., Dubois-Fernandez, P., Dupuis, X. (2008): "Information theory-based approach for contrast analysis in polarimetric and/or interferometric SAR images", *IEEE Trans. Geosci. Remote Sens.*, 46(8), pp. 2185–2196.

Mulder, V.L., Bruin, S. de, Schaepman, M.E., Mayr, T.R. (2011): "The use of remote sensing in soil and terrain mapping: a review", *Geoderma*, 162, pp.1–19.

Paruelo, J.M., Beltrán, A.B., Jobbagy, E.G., Sala, O.E., Golluscio, R.A. (1998): "The climate of Patagonia: General patterns controls on biotic processes", *Ecología Austral*, 8, pp. 85–101.

Pottier, E., Ferro-Famil, L., Allain, S., Cloude, S.R., Hajnsek, I., Papathanassiou, K., Moreira, A., Williams, M., Minchella, A., Lavalle, M., Desnos, Y.L. (2009): "Overview of the PolSARpro v4.0: The open source toolbox for polarimetric and interferometric polarimetric SAR data processing", in *Proc. Int. Geosci. Remote Sens. Symp.*, pp. 936–939.

Prigent, C., Tegen, I., Aires, F., Marticorena, B., Zribi, M. (2005): "Estimation of the aerodynamic roughness length in arid and semi-arid regions over the globe with the ERS scatterometer", *J. Geophys. Res.*, 110, pp. 1–12.

Del Valle, H., Hardtke, L., Blanco, P. y Sione, W. (2013): "Assessment of land degradation Using Shannon entropy Approach On Polsar Images In Patagonian Coastal deserts", GeoFocus (Artículos), nº13-2, p. 84-111. ISSN: 1578-5157

Qong, M. (2000): "Sand dune attributes estimated from SAR images", *Remote Sensing Environment*, 74, pp. 217–228.

Ray, T.W., Farr, T.G., van Zyl, J.J. (1992): "Detection of land degradation with polarimetric SAR", *Geophysical Research Letters*, 19(15), pp. 1587-1590.

Rosenqvist, A., Shimada, M., Ito, N., Watanabe, M. (2007): *"ALOS PALSAR: a pathfinder mission for global-scale monitoring of the environment", IEEE Trans. Geosci. Remote Sens.*, 45, pp. 3307–3316.

Rostagno, C.M. (1981): *Reconocimiento de suelos de Península Valdés*. Contribution no. 44. CENPAT (CONICET), Puerto Madryn, Chubut, Argentina.

Sahai, B. (1993): *"Remote sensing of deserts: the Indian experience", Journal of Arid Environments*, 25, pp. 173-185.

Schaber, G.G. (1999): "SAR studies in the Yuma Desert, Arizona: San penetration, Geology, and the detection of military ordnance debris", *Remote Sens. Environ.*, 67, pp. 320–347.

Schaber, G.G., Breed, C. (1999): "The Importance of SAR Wavelength in Penetrating Blow Sand in Northern Arizona", *Remote Sensing of the Environment*, 69, pp. 87-104.

Shimada, M. *et al.* (2006): "PALSAR initial calibration and validation results", *Proc. SPIE*, 6359–6367.

Stephen, H., Long, D.G. (2004): "Analysis of scatterometer observations of Saharan Ergs using a simple rough facet model", *IEEE Trans. Geosci. Remote Sens.*, pp. 1534–1537.

Tueller, P.T., Lorain, G. (1973): *Application of remote sensing techniques for analysis of desert biome validation studies*. Utah State University. US/IBP Desert Biome Digital Collection.

Van Zyl, J., Arii, M., Kim, Y. (2011): *"Model-based decomposition of polarimetric SAR covariance matrices constrained for nonnegative eigenvalues", IEEE Transactions on Geoscience and Remote Sensing*, 49, 9, pp. 3452-3459.

Zárate, M.A., Tripaldi, A. (2012): "The aeolian system of central Argentina", *Aeolian Research* 3, pp. 401-417.